Journal of Molecular Structure 1137 (2017) 720–724

Contents lists available at ScienceDirect

Journal of Molecular Structure

journal homepage: http://www.elsevier.com/locate/molstruc

The influence of Ni(II) on brushite structure stabilization

J.R. Guerra-López [a, *], J.A. Güida [a, b], M.A. Ramos [a], G. Punte [c]

[a] Departamento de Ciencias Básicas, Universidad Nacional de Luján, rutas 5 y 7, Luján, Argentina
[b] CEQUINOR, Departamento de Química, Facultad de Ciencias Exactas, Departamento de Ciencias Básicas, Facultad de Ingeniería, Universidad Nacional de La Plata, CC 962, 1900, La Plata, Argentina
[c] IFLP y LANADI, Departamento de Física, Facultad de Ciencias Exactas, Universidad Nacional de la Plata, CC 67, 1900, La Plata, Argentina

ARTICLE INFO

Article history:
Received 30 December 2016
Received in revised form
20 February 2017
Accepted 20 February 2017
Available online 22 February 2017

Keywords:
Brushite
Urinary calculi
Calculi phosphate
Infrared spectroscopy
Powder X-ray diffraction

ABSTRACT

Brushite samples doped with Ni(II) in different concentrations, from 5% to 20%, were prepared in aqueous solution at pH = 7 and at two temperatures: 25 and 37 °C. The solid samples were characterized by chemical analysis, infrared spectroscopy (FTIR) and x-ray powder diffraction (XRPD). Chemical analysis has shown Ni(II) almost complete incorporation to the solid phase up to 15%. X-ray diffraction patterns have allowed to identify brushite phase with almost no modification of the line breadth and only small shifts of lines positions with increasing Ni(II) incorporation up to 15%. For larger Ni(II) concentration, in solution, a mixture of phases has been detected. Infrared spectra have supported diffraction results. For Ni(II) 20% and over the characteristic bands of HPO_4^{2-} anions tend to vanish, and the typical shaped PO_4^{3-} bands are observed. These results have allowed to establish that the presence of low levels of Ni in the synthetic process not only helps brushite formation; but, also prevents brushite from apatite conversion and, in addition, preserves brushite crystallinity. According to these findings, it is possible to propose that nickel traces present in the urinary system might be a trigger to brushite stone formation and/or growth, rather than the expected brushite conversion to hydroxyapatite. This outcome would explain the recurrent detection of difficult to treat brushite stones, observed in the last three decades.

1. Introduction

Urinary calculi precipitate in the urinary tract of human and animals as consequence of a number of health disorders. Several statistical studies in humans, performed in different countries, had shown that the prevalence of kidney stones has increased over the last three decades and that one of three stone formers experienced recurrence with the consequent costly, painful and chronic healthcare problem [1]. Another finding of care providers and researchers was related with modifications in stones composition. It was determined that Ca(II) cation is involved in 85% of the found stones, mainly in the form of oxalate (CaOx) admixed with some form of calcium phosphates (CaP), especially apatite and brushite ($CaHPO_4 \cdot 2H_2O$, calcium monohydrogen phosphate dihydrate). 25% of CaP patients form brushite stones. These stones have been found aggressive, difficult-to-treat and recurrent, with increase proportion of brushite in calculi composition [2]. Several surveys and researches have been performed in the last decade addressing biochemical, physicochemical and physiological conditions of brushite stone patient, trying to find ways to deal with them [3–6]. According to several authors hypercalciuria, a diminished citrate excretion and an elevated urine pH increase stone risk. While low sodium diets and thiazide-type diuretics potentially reduce stone recurrence, see for example refs. [1,5]. Though no clear and unique factor can be related to prevention of calculi reappearance in the case of idiopathic renal stones all the above mentioned studies indicate that knowledge of their composition is an important, and sometimes the only tool to identify disorder origin [7–9] or more appropriate ways of treatment. Therefore, the analysis must be performed under reliable analytical methods [9–11].

Other approaches have also been tried to improve stone treatment. They have been related with the study of the influence of different elements or ambient conditions in phases present in urinary stones, with the microelemental composition of CaP or with the stabilization and grain growth of brushite [12–14].

In this work, we try to add to the knowledge of brushite formation and stabilization in controlled conditions. In previous work,

* Corresponding author.
E-mail addresses: joseguerralopez1@gmail.com, jguerra@unlu.edu.ar (J.R. Guerra-López), guida@quimica.unlp.edu.ar (J.A. Güida), gmpunte@gmail.com (G. Punte).

http://dx.doi.org/10.1016/j.molstruc.2017.02.076
0022-2860/

we had studied the influence of foreign metal ions on calcium phosphate crystallization and their incidence on biological mineralizations. From those studies we found out that calcium hydroxyapatite (CaHAP) can be thermally stabilized by Ca(II) substitution by Zn(II) [15], while could not crystallize in presence of Ni(II) [16].

Here we are presenting the investigation of the effects of Ni(II) on the transformation of brushite to CaHaP and relating this with the development of kidney stones. Samples were characterized by atomic absorption (A.A.), x-ray powder diffraction (XRPD) and infrared spectroscopy (FTIR). The results are presented below.

2. Experimental

2.1. Brushite synthesis

Brushite was prepared by the method of Tovborg-Jensen and Rathlev [17]. A solution containing $Na_2HPO_4 \cdot 8H_2O$ and KH_2PO_4 and a solution containing $CaCl_2 \cdot 6H_2O$ both 0.1 M were prepared. These solutions were added simultaneously at the same rate to a constantly stirred solution containing KH_2PO_4 0.1 M at 25 °C. The addition rates were maintained in order to keep the pH at 4.8. The solid was filtered, washed with H_3PO_4 0.05% and dried at 60 °C.

2.2. Brushite synthesis doped with Ni(II) cations

The preparation method was adapted from a previous hydroxyapatite synthetic procedure [15]. The phosphates were prepared by dropwise addition of two solutions 0.2 M (one of calcium and nickel acetate and other of ammonium phosphate) to a stirred solution of ammonium acetate. The amount of $[H_3O^+]$ in solution changes during the synthesis. Then, to keep the pH of the solutions at the constant value of 7, NH_3 or acetic acid 0.1 M were added; pH measurements were made with an MV 870 digital pH meter and using a combined glass electrode. The electrode was calibrated at 25 °C with a buffer prepared according to the National Bureau of Standards [15]. After the above procedure, the synthesized phosphates were kept into a water bath for 24 h at 25 °C (or 37 °C) and pH 7.

The composition of the solution was varied in steps, from pure calcium acetate to 20% of Ni and 80% of calcium acetate. The upper range of [Ni/Ca] ratio in the solution was selected based on a previous study [16], which showed that nickel concentrations of 20% and over induced formation of mixed phases. The solid samples obtained were named by the nickel symbol followed by a number (n) (Nin), which indicated the nickel concentration in the solution expressed as percent.

The composition of the products was checked by determination of Ca, Ni and P content. Ca and Ni were determined by atomic absorption spectrometry and phosphorus was determined spectrophotometrically. The solid phases obtained from [Ni/Ca] molar ratio solutions ranging from 5% to 20%, at 25 °C and 37 °C, were analyzed by FTIR and XRPD, as the rest of samples previously studied [16].

FTIR spectra of powdered samples in the form of pressed KBr pellets were measured with a Bruker IFS 66 FTIR spectrometer in the range 4000–400 cm^{-1} (4 cm^{-1} resolution).

The X-ray diffraction data were obtained with a Philips PW1710 powder diffractometer with a scintillation counter and an exit beam graphite monochromator using CuKα radiation ($\lambda = 1.5406$ Å). The 2θ range covered was: $7 \leq 2\theta \leq 120°$, with a step interval of 0.02° and a counting time of 5s.

3. Results and discussion

3.1. Chemical analysis

The results of the chemical analysis of the synthesized (Ca,Ni) $HPO_4 \cdot 2H_2O$ samples are collected in Table 1. The molar (Ca + Ni)/P ratio found in the solid was in the range of 0.97–1. Analysis of data of Table 1 shows that nickel incorporation in the solid is almost complete from Ni5 to Ni15 (82%). For Ni20 sample, however, the (Ca + Ni)/P ratio is higher than 1. This behavior is attributed to the coexistence of phases. (see spectroscopic and diffraction results below).

3.2. X-ray diffraction results

The obtained XRPD patterns of brushite and (Ni,Ca)$HPO_4 \cdot 2H_2O$ samples synthesized at 25 °C are shown in Fig. 1. Diffraction lines observed in this figure only showed a small variation in position and breadth with increasing Ni(II) concentrations up to Ni 15%. This indicated that neither loss of crystallinity nor new phases formation have been caused by Ni incorporation. For Ni(II) concentration in solution higher that 15%, the contribution of brushite to the pattern drastically diminishes, see Ni20 in Fig. 1, and other phase starts to form.

Following Curry and Jones structural model for brushite [18] the XRPD patterns of samples Nij ($j \leq 15$) could be fitted assuming the monoclinic non centrosymmetric space group Cc. The structure can be described as sheets perpendicular to the ***b*** axis linked by waters' hydrogen bonds (HB), as shown in Fig. 2. Calcium (or Ca,Ni) cations are coordinated by eight oxygen atoms, two from the two crystallographically inequivalent water molecules and the remaining six from the phosphate anions. The resulting dodecahedron polyhedra shear two edges and build infinite zigzag chains along ***c*** axis as shown in Fig. 2B. Chains are connected by the tetrahedral phosphate anions forming the mentioned sheets.

The inequivalent water molecules show some differences in the strengths of their HB. The HB connecting the layers show in both molecules the same OH···O length value (d) within 3 e.s.d.s, mean d = 2.805(5) Å. Whereas the HB linking oxygen atoms within the same layer exhibits an appreciable d value difference, $d_{W1} = 2.76(1)$Å and $d_{W2} = 3.08(1)$ Å. It should be noticed that W2 HB acceptor is the hydroxyl O atom.

3.3. Infrared spectra

Fig. 3 compares the infrared spectra of synthesized samples in different Ni(II) concentrations, from Ni5 to Ni20 at 25 °C. It can be seen from it, in agreement with X-ray diffraction results, that from Ni5 to Ni15 small and continuous changes can be observed, but for concentrations greater than 15% a mixture of phases tends to form. The FTIR spectra of samples obtained at 37 °C are not shown because no appreciable differences were observed.

Table 2 summarizes the assignments of infrared fundamental modes for brushite and (Ca,Ni)$HPO_4 \cdot 2H_2O$. All assignments are consistent with those observed by other authors [17,19,20]. Due to the small differences observed in the band positions coming from samples Ni5 to Ni15, only data from sample Ni5 were included in this table.

The O–H stretching mode appeared in a wide spectral region 3700-3200 cm^{-1} for the phase brushite. The inequivalence of water molecules -pointed out before from the crystal structure analysis- was also evidenced by the splitting of the antisymmetric mode (ν_3) of the two water molecules at 3545, and 3490 cm^{-1}. The splitting of the symmetric one (ν_1) was also observed at 3280 and 3169 cm^{-1}. Since W1 forms stronger H-bonds, according to the bond distances

Table 1
Inclusion of Ni(II) in solid phase.

Initial Ni(II) in preparation		Synthesis results			
x = Ni (% in mol)[a]	Ni (% in wt)	Ni in solid (% in wt)[b]	Ni in solid (% in wt)	Ni in solid (% in wt)[b]	Ni in solid (% in wt)[b]
5	3.0	2.8 ± 0.1	97.0	3.0	1
10	5.9	5.2 ± 0.1	88.0	12.0	0.98
15	8.8	7.2 ± 0.1	82.0	18.0	0.95
20	NC[c]	NC[c]	NC[c]	NC[c]	Mixture

[a] Initial Ni concentration before reaction, calculated by: Ni/(Ca + Ni)*100; x is related to brushite formula: $Ca_{(10-x)}Ni_xPO_4 \cdot 2H_2O$.
[b] Ni concentration was quantified by atomic absorption (AA).
[c] Not calculated because mixed phases have been formed (see vibrational spectra discussion).

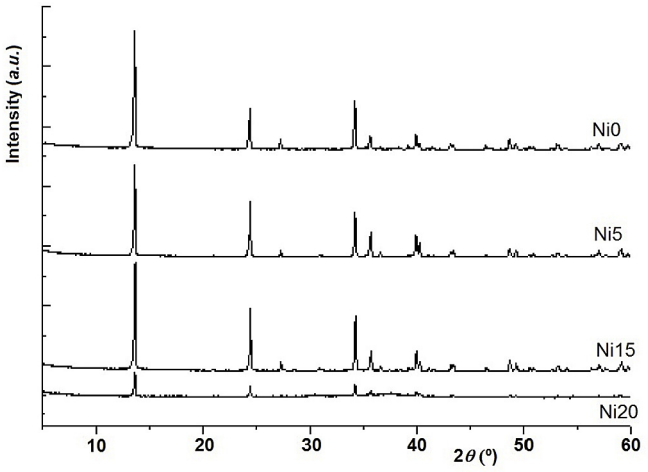

Fig. 1. X-ray diffraction patterns for (Ca,Ni)$HPO_4 \cdot 2H_2O$ samples with different Ni percentages Ni 0% (brushite), Ni 5%, Ni 15%, and Ni 20% (curves were taken from samples obtained at 25 °C, curves at 37 °C have not shown differences).

described above, the ν_3-ν_1 set for this molecule should be assigned to the lowest frequency bands (3490-3169 cm^{-1}), while for the W2 the corresponding bands should be assigned to the remaining set at 3545-3280 cm^{-1} because this molecule presented the longest H-bonds. The band profile of this region suffers a gradual change with the increase of Ni(II) concentration in the samples up to Ni15.

It can also be seen from Table 2 that the incorporation of nickel provokes a band shift of the modes corresponding to phosphate ion and $\nu(OH)_{H2O}$. The continuous shifts observed in bands spectra for samples Ni5 to Ni15 drastically changed when passing to Ni20. The stretching bands of water at about 3500 cm^{-1} miss their fine structure described above, and the typical antisymmetric stretching (ν_3) bands of phosphate appeared at about 1100 cm^{-1}. At the same time, small components of HPO_4^{2-} bands were still observed in Ni20. These spectroscopic results were in agreement with X-ray diffraction findings.

Present XRPD and FTIR results have allowed to establish that the presence of low levels of Ni(II) in the synthetic process not only helps brushite formation; but, also prevents brushite from apatite conversion and, in addition, preserves brushite crystallinity. While, in similar conditions in absence of nickel previous studies have evidenced that, at neutral pH and a temperature of 25 °C the formation of hydroxyapatite was favoured [11,16].

These findings seem to be at least controversial in view of the fact that brushite has been considered a precursor phase of hydroxyapatite [7,10,11,21,22] and that for this reason

dicalcium phosphate cements were developed two decades ago, and ever since there has been a substantial growth in research aimed to the improvement of their properties in order to satisfy the requirements for different clinical applications.

However, the formation of brushite in synthetic and biological systems are governed by factors such as the nature of the media: pH, temperature and the presence of trace elements [14,16,19], which prevent brushite from convert to hydroxyapatite. If this conversion does not happen in the urinary system, brushite stones would form. Unlike hydroxyapatite, which fragments easily, brushite stones are exceptionally hard and difficult to remove surgically [7,10,11,23].

As, Krambeck et al. [6] had reported, the calcium phosphate stone disease is increasing; specifically brushite stone disease has

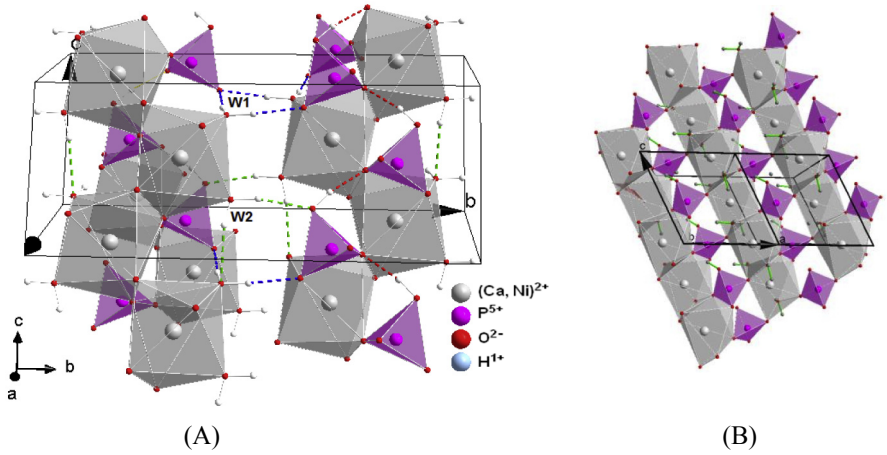

Fig. 2. Brushite crystal packing. A) It shows (Ca,Ni) coordination polyhedra and monohydrophosphate tetrahedra. W1 hydrogen bonds in blue, W2 hydrogen bonds in green, and acidic hydrogen bonds in red. B) View of the packing up ***b***. (For interpretation of the references to colour in this figure legend, the reader is referred to the web version of this article.)

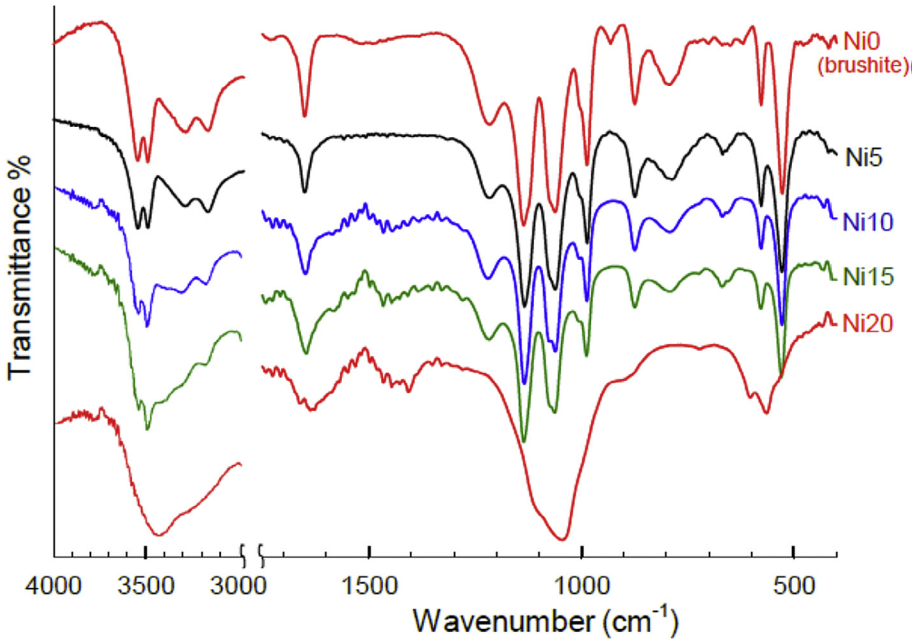

Fig. 3. Infrared spectra of $(Ca,Ni)HPO_4 \cdot 2H_2O$ with different Ni percent: Ni 0% (brushite), Ni 5%, Ni 10%, Ni 15% and Ni 20% (spectra were taken from samples obtained at 25 °C).

Table 2
Observed infrared bands (cm^{-1}) for Brushite and $(Ca,Ni)HPO_4 \cdot 2H_2O$ (Ni5) and its assignment (Data from samples obtained at 25 °C).

Mode	$CaHPO_4 \cdot 2H_2O$	$(Ca,Ni)HPO_4 \cdot 2H_2O$ (Ni5)
$\nu_3(H_2O)$	3545s, 3490s	3536 s, 3489 s
$\nu_1(H_2O)$	3280 s, 3169 s	3302 w, 3167 s
ν(PO–H)	2930 sh, 2380 w, 2270 sh	2400 vw, 2268 w
$\delta(H_2O)$	1648	1648
δ(PO–H)	1215 w, 1200 sh	1218 s
ν_d(P–OH)	1140s, 1123 sh, 1075 sh, 1057 s	1134 s, 1121 sh, 1074 sh, 1063 s
ν_s(P–OH)	1000 sh, 984 s	987 s, 1004 sh
ν(P–O(H))	875 s	875 s
δ(P–O(H))	785 vw	792 w
Waters libration	665 vw, 663 w	670 m, 653 wh
δ(O–P–O(H))	583 w	576 s
δ(O–P–O(H))	535 sh, 519 w	527 s
δ(O–P–O(H))	417 w	430 w

vs: very strong, s: strong, m: medium, w: weak, vw: very weak, sh: shoulder.

been shown to be on the rise. Furthermore, these authors have found evidence to support some correlation between brushite stone disease and previous calcium oxalate stone treatment.

Recent investigations have found that brushite may play crucial roles in oxalate renal stones formation [24], however latest research [[25] and references therein] seems to indicate that is unlike that brushite may promote oxalate stones, but found that amorphous calcium phosphate is central in the nucleation of calcium oxalate. Both results are compatible with our results on the role of Ni in the formation of different phosphates.

Taking into account the results presented in this work, that Ni presence in human beings as contaminant is not infrequent and that it primary accumulates in lungs and kidneys, it seems reasonable to propose that nickel traces present in the urinary system may trigger brushite stone formation, with the possible development of these stones rather than their conversion to hydroxyapatite. Nickel may also favor the presence of amorphous calcium phosphate [16] helping oxalate nucleation as determined by Xie et al. [25].

4. Conclusions

We have investigated the effect of nickel on brushite crystals formation by x-ray diffraction and FTIR. Results coming from both techniques showed that under the synthesis conditions (neutral pH and at two different temperatures: 25 and 37 °C) only one phase is formed when up to a 15% of Ni(II) is included in phosphate synthesis. For larger Ni(II) concentration in solution other phases are formed as can be seen from the diminution of the contribution of brushite to the obtained XRDP pattern and the observation in the FTIR spectra of the typical tetrahedral phosphate bands and loss of the fine structure of water stretching bands.

Present results would have some biological implications as they suggest that brushite kidney stones may develop as results of presence of traces of Ni(II) in biological fluids and that Ni(II) traces may also induce amorphous calcium phosphate formation, which facilitates calcium oxalate nucleation.

In future work we are planning to synthesize different calcium phosphates from simulated biological fluids. To characterize the solid materials to be obtained we have designed a set of experimental techniques to validate our present assumptions.

Acknowledgements

The authors acknowledge National Scientific and Technological Research Council of Argentina (CONICET) projects: PIP0985 and PIP03272; Universidad Nacional de La Plata (UNLP, Argentina) projects: 11X/577, 11X565, 11X672 and 11X/7093, Departamento de Ciencias Básicas de la Universidad Nacional de Luján (UNLu, Argentina) projects B112 and B152 and SNRX and CONICET (Projects M6 and AC7) for financial support. J.A.G and G.P. are members of the research staff of CONICET.

References

[1] F.L. Coe, E.M. Worcester, A.P. Evan, Idiopathic hypercalciuria and formation of calcium renal stones, Nat. Rev. Nephrol. 12 (2016) 519–533 (and references

therein).
[2] N. Mandel, I. Mandel, K. Fryjoff, T. Rejniak, G. Mandel, Conversion of calcium oxalate to calcium phosphate with recurrent stone episodes, J. Urol. 169 (2003) 2026–2029.
[3] C.Y. Pak, J.R. Poindexter, R.D. Peterson, H.J. Heller, Biochemical and physicochemical presentations of patients with Brushite stones, J. Urol. 171 (2004) 1046–1049.
[4] A.E. Krambeck, S.E. Handa, A.P. Evan, J.E. Lingeman, Profile of the brushite stone former, J. Urol. 184 (2010) 1367–1371.
[5] R. Siener, L. Netzer, A. Hesse, Determinants of brushite stone formation: a case- control study, Plos One 8 (11) (2013) e78996, 6pp.
[6] A.E. Krambeck, S.E. Handa, A.P. Evan, J.E. Lingeman, Brushite stone disease as a consequence of lithotripsy? Urol. Res. 38 (2010) 293–299.
[7] A. Hesse, D. Heimbach, Causes of phosphate stone formation and importance of metaphylaxis by urinary acidification: a review, World J. Urol. 17 (1999) 308–3015.
[8] I.A. Abboud, Concentration effect of trace metals in Jordanian patients of urinary calculi, Environ. Geochem Health 30 (2008) 11–20.
[9] J. Guerra-López, J.A. Güida, C.O. Della Védova, Infrared and Raman studies on renal stones: the use of Second derivative infrared spectra, Urol. Res. 38 (2010) 383–390.
[10] D. Bazin, M. Daudon, C. Combes, C. Rey, Characterization and some physicochemical aspects of pathological microcalcifications, Chem. Rev. 113 (2012) 5092–5120.
[11] J.R. Guerra-López García, J.A. Güida, Aplicación de la espectroscopia IR en el estudio de la composición de cálculos renales, Editorial Académica Española, Saarbrücken, Germany, 2012.
[12] T.N. Moroz, N.A. Palchik, A.V. Dar, Nuclear instruments and methods in physics research section a: accelerators, spectrometers, Detect. &Assoc. Equip. 603 (2009) 141–143.
[13] H.E. Lundager Madsen, Influence of foreign metal ions on crystal growth and morphology of brushite ($CaHPO_4$, $2H_2O$) and its transformation to octacalcium phosphate and apatite, J. Cryst. Growth 310 (2008) 2602–2612.
[14] A.M. Matthew, R.K. Matthew, K.J. Manoj, R.L. Preston, A.S. Madden, A. Cuneyt Tas, Testing of Brushite ($CaHPO_4.2H_2O$) in synthetic biomineralization solutions and *in Situ* crystallization of Brushite micro-granules, J. Am. Ceram. Soc. 95 (2012) 2178–2188.
[15] J.R. Guerra-López, G.A. Echeverría, J.A. Güida, R. Viña, G. Punte, Synthetic hydroxiapatites doped with Zn(II) studied by X-ray diffraction, infrared, Raman and thermal analysis, J. Phys. Chem. Solids 81 (2015) 57–65.
[16] J. Guerra-López, R. Pomés, C.O. Della Védova, R. Viña, G. Punte, Influence of nickel on hydroxyapatite crystallization, J. Raman Spectrosc. 32 (2001) 255–261.
[17] A. Tovborg-Jensen, J. Rathlev, Vibration spectra of brushite, $CaHPO_4.2H_2O$, Inorg. Syn. 4 (1953) 19–24.
[18] N.A. Curry, D.W. Jones, Crystal structure of brushite, calcium hydrogen orthophosphate dihydrate: a neutron-diffraction investigation, J. Chem. Soc. A (1971) 3725–3729.
[19] J.C. Elliot, Structure and Chemistry of Apaptites and Other Calcium Orthophosphates, Elsevier, Amsterdam, London, New York, Tokyo, 1994.
[20] D. Bazin, P. Chevallier, G. Matzen, P. Jungers, M. Daudon, Heavy elements in urinary stones, Urol. Res. 35 (2007) 179–184.
[21] W.F. Neman, T.Y. Toribara, B.J. Mulryan, Synthetic hydroxyapatite crystals. 1. Sodium and potassium fixation, Arch. Biochem. Biophys. 98 (1962) 384–390.
[22] B.R. Matlaga, F.L. Coe, A.P. Evan, J.E. Lingeman, The role of Randall's plaques in the pathogenesis of calcium stones, J. Urol. 177 (2007) 31–38.
[23] F. Tamimi, Z. Sheikh, J. Barralet, Dicalcium phosphate cements: brushite and monetite, Acta Biomater. 8 (2012) 474–487.
[24] R. Tang, G.H. Nancollas, J.L. Giocondi, J.R. Hoyer, C.A. Orme, Dual roles of brushite crystals in calcium oxalate crystallization provide physicochemical mechanisms underlying renal stone formation, Kidney Int. 70 (2006) 71–78.
[25] B. Xie, T.J. Halter, B.M. Borah, G.H. Nancollas, Aggregation of calcium phosphate and oxalate phases in the formation of renal stones, Cryst. Growth Des. 15 (2015) 204–211 (and references therein).